Solid State Phenomena Vols 233-234 (2015) pp 179-182
© (2015) Trans Tech Publications, Switzerland
doi:10.4028/www.scientific.net/SSP.233-234.179

Submitted: 2014-06-20
Revised: 2014-11-06
Accepted: 2014-11-07

Annealing influence on the exchange-bias and magnetostructural properties in the $Ni_{50.0}Mn_{36.5}Sn_{13.5}$ ribbon-shape alloy

L. González-Legarreta[1*], M. Ipatov[2], D. González-Alonso[3], A. P. Kamantsev [4], V. V.Koledov[4], V. G. Shavrov[4], B. Hernando[1].

[1]Dept. de Física, Universidad de Oviedo, Calvo Sotelo s/n, 33007 Oviedo, Spain
[2]Department of Materials Physics, Faculty of Chemistry, University of the Basque Country, San Sebastian 20018, Spain.
[3]Facultat de Física, Departament d'Estructura i Constituents de la Matèria, Universitat de Barcelona, Diagonal 647, E-08028 Barcelona, Spain
[4]Kotelnikov Institute of Radio Engineering and Electronics of RAS, Moscow 125009, Russia.
*lorena.glegarreta@gmail.com

Keywords: Heusler alloys, martensitic transformation, exchange-bias, Ni-Mn-Sn.

Abstract: We report on the influence of short annealing treatments at 923 K and 1073 K during 10min on both martensitic transformation and exchange bias effect for the $Ni_{50.0}Mn_{36.5}Sn_{13.5}$ Heusler alloy ribbon by means of magnetic measurements. We have observed that the martensitic transformation is shifted towards higher temperatures with increasing annealing temperature. Furthermore, isothermal *M(H)* hysteresis loops performed under field-cooling protocol show an exchange bias effect for as-quenched and two annealed ribbons, which indicates the existence of ferromagnetic-antiferromagnetic interactions at low temperatures. In particular, we observe that H_C diminishes with the increasing of the annealing temperature, but H_E is not affected by the heat treatment.

Introduction

Over the last decades, the study of Mn-rich $Ni_{50}Mn_{50-x}Z_x$ (Z = Sb, Sn and In) Heusler alloy systems have attracted great attention due to their multifunctional properties such as magnetic shape memory effect [1], large magnetocaloric effect (MCE) [2], giant magnetoresistance [3,4] or exchange bias effect (EB) [5]. Most of these functional properties are associated with a strong magneto-structural coupling, being the valence electron concentration (*e/a*) a key factor [6, 7]. However, the EB effect, described as the shift of the magnetic hysteresis loop of a material from the origin when it is cooled in the presence of an applied magnetic field [8], is related with the Ferromagnetic (FM)-Antiferromagnetic (AFM) coupling at low temperatures in the martensitic state [9]. This could be associated with the Mn-excess atoms, which could occupy Ni or *Z* sites, and are antiferromagnetically coupled to Mn atoms at regular sites [10]. In this work, we report the annealing influence on both martensitic transformation and exchange bias effect on $Ni_{50.0}Mn_{36.5}Sn_{13.5}$ Heusler alloy ribbon.

Experimental

The polycrystalline $Ni_{50.0}Mn_{36.5}Sn_{13.5}$ Heusler alloy was performed by arc-melting technique, employing highly pure elements (> 99.98%) and produced in ribbon-shape by rapid solidification using the melt-spinning method at 48 m/s under Ar atmosphere. Ribbon flakes were obtained with 7–12 μm in thickness, 2.0 mm in width and 4–12 mm in length. In order to study the annealing influence on both martensitic transformation and exchange bias effect for this alloy, a piece of sample was kept as reference (as-quenched ribbon) and some pieces of the same ribbon were annealed for 10min at 923 K and 1073 K. The annealing was performed in vacuum quartz tubes and tantalum foil was used for wrapping each sample before introducing it in the quartz container for avoiding Si contamination. The quartz tubes, containing the ribbons to be treated, were introduced in the quartz furnace after reaching the appropriate annealing temperature. Ribbon-flakes were then quenched in ice water. The morphology and the average composition for all the ribbon samples were performed by means of Scanning Electron Microscopy (SEM-JEOL6100) equipped with an

Energy Dispersive X-ray microanalysis system (EDX-Inca Energy 200). From latter analyses we obtain an average composition of $Ni_{50.3}Mn_{36.5}Sn_{13.2}$ for both as-quenched and annealed ribbon at 923 K, and $Ni_{48.3}Mn_{38.6}Sn_{13.1}$ for the annealed ribbon at 1073 K. The estimated error in determining the concentration of each element is of ±0.1 %. The magnetic measurements were done under Zero-Field-Cooling (ZFC), Field-Cooling (FC) and Field-Heating (FH) protocols by Vibrating Sample Magnetometer (VSM, VersaLab QD) in the range of 50 – 400 K and at an applied magnetic field ranging from 50 Oe up to 30 kOe. The heating and cooling rates were of 5 K/min. *M(H)* Hysteresis loops were measured within the temperatures range from 5 K to 300 K by a Physical Property Measurement System (PPMS-9, QD).

Results and Discussions

The ZFC, FC and FH thermomagnetic curves recorded at different applied magnetic fields for the as-quenched ribbon are shown in Fig.1. At high temperatures and low magnetic fields, in the austenite state, the sample is paramagnetic and orders ferromagnetically below T_c^A = 312 K. Just below the Curie point T_C^A, it is detected a maximum in the magnetization, which is related to the Hopkinson effect [11]. In the temperature range from 250 to 310 K the FC and ZFC curves display a thermal hysteresis ΔT, indicating a First-Order Structural-Transformation (FOST) from austenite to martensite phase. The characteristic transformation temperatures, martensite start and finish (M_s, M_f) and austenite start and finish (A_s, A_f) are collected in Table 1. Below the FOST, at T_C^M = 246 K, the as-quenched sample undergoes a magnetic transition associated with the magnetic state of the martensite phase, which becomes ferromagnetic. Below T_C^M, a splitting between the ZFC and FC curves is observed at low fields. This feature has also been observed in other Ni–Mn–Sn Heusler alloy systems, which is associated with the coexistence of Antiferromagnetic (AFM) and Ferromagnetic (FM) interactions at low temperatures [5,6,9]. In fact, the latter give rises to an exchange-bias effect as will be shown below. Moreover, the M_s decreases with increasing the applied magnetic field stabilizing the austenitic phase.

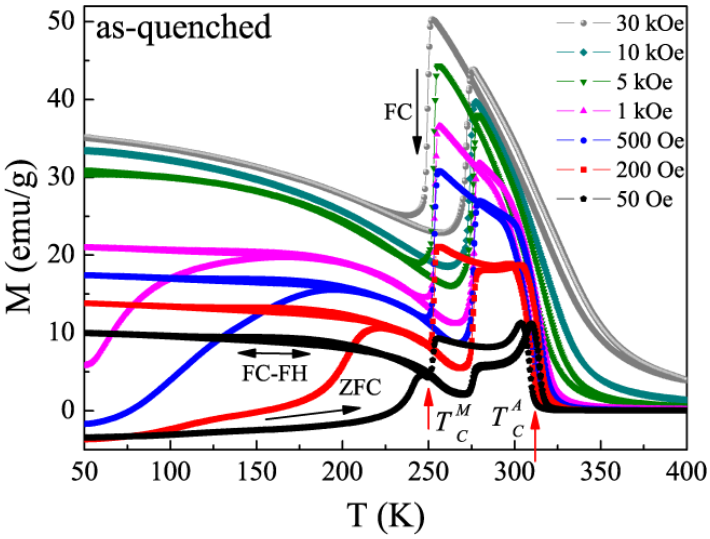

Figure 1: Thermomagnetic curves *M(T)* for as-quenched $Ni_{50.0}Mn_{36.5}Sn_{13.5}$ alloy ribbon obtained at different magnetic fields. Black arrows are indicative for cooling and heating runs in ZFC, FC, and FH protocols, while red vertical arrows point at the Curie temperatures for martensitic and austenitic states.

Fig. 2 (a) and (b) show a comparison among the thermomagnetic measurements at 200 Oe and 30 kOe for the three samples. After annealing, it is observed a shift of the martensitic transformation towards higher temperatures, which signifies the stabilization of the martensite phase at the expense of the parent one. The corresponding structural martensitic temperatures for the annealed ribbons along with the as-quenched one are collected in Table 1.

Sample	M_s (K)	M_f (K)	A_s (K)	A_f (K)	ΔT (K)	T_C^A (K)
As-quenched	258	250	270	275	17	312
Ann 923 K	271	259	277	290	19	312
Ann 1073 K	278	266	284	299	21	306

Table 1: Martensitic structural temperatures for of as-quenched and annealed $Ni_{50.0}Mn_{36.5}Sn_{13.5}$ ribbons at 923 K and 1073 K determined by *M(T)* measurements.

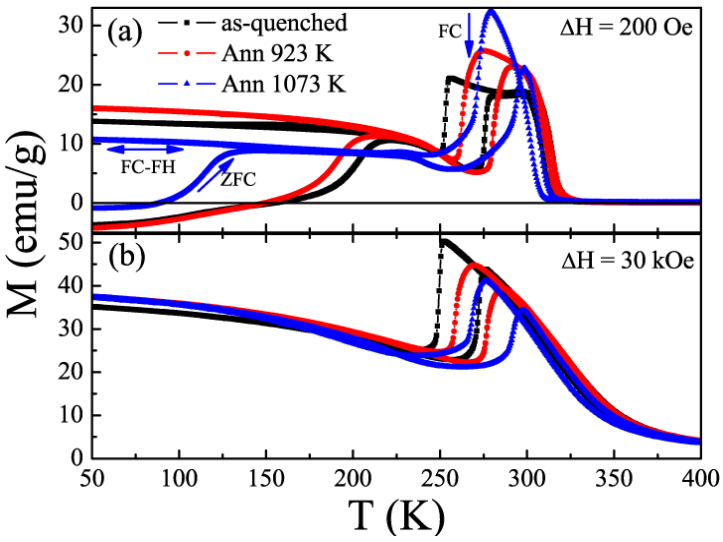

Figure 2: Magnetization temperature dependence *M(T)* obtained at a field of 200 Oe (a) and 30 kOe (b) for as-quenched and annealed $Ni_{50.0}Mn_{36.5}Sn_{13.5}$ alloy ribbons. Blue arrows are indicative for cooling and heating runs in ZFC, FC, and FH protocols.

Furthermore, in comparison with the as-quenched and the Ann 923 K samples that show the same magnetic transition temperature T_C^A at the austenitic-phase, for the corresponding one to the Ann 1073 K sample the T_C^A decreases. This can be explained by the shift in the compositions, since the Ann 1073 K ribbon has more Mn content than the other ones. For Ni–Mn–Sn Heusler alloys, it is well known that T_C^A is mainly determined by the ferromagnetic Mn-Mn interaction strength, while the Mn-excess content leads to an antiferromagnetic coupling with the Mn located at the Ni/Sn sites, which in turn reduces the strength of the ferromagnetic interactions. As a result, the T_C^A decreases with increasing Mn content [12]. Moreover, in Fig. 2 (a), we observe that the annealed ribbons display a splitting between the ZFC and FC curves, which suggests a FM-AFM coupling at low temperatures [6].

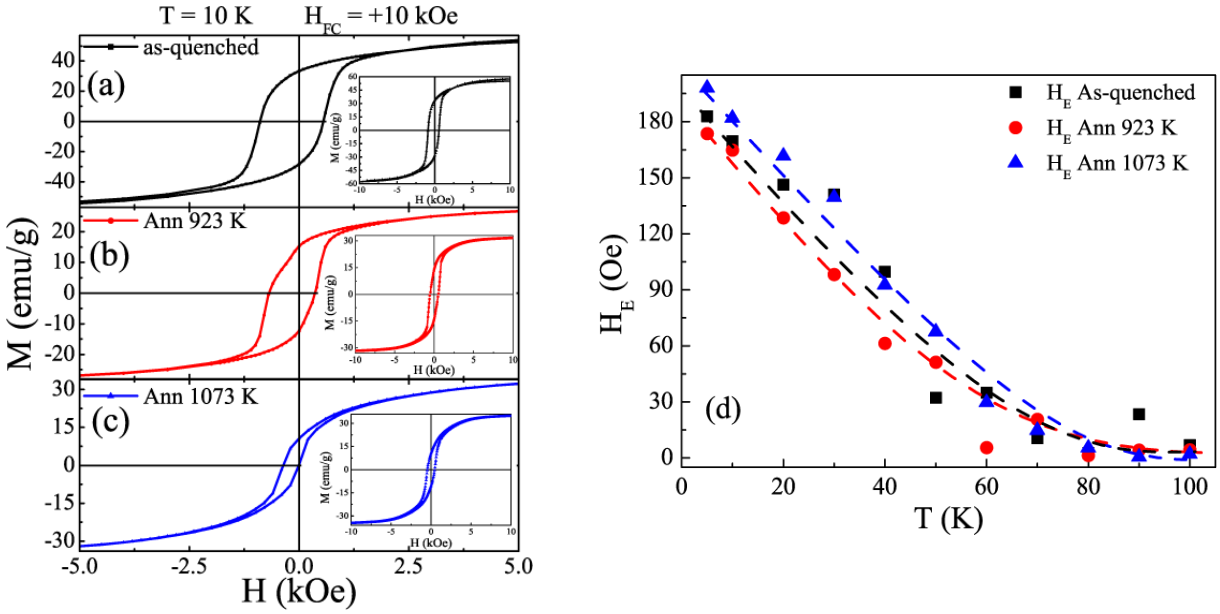

Figure 3: Isothermal magnetization hysteresis loops for as-quenched and for annealed $Ni_{50.0}Mn_{36.5}Sn_{13.5}$ alloy ribbons performed at 10 K after FC (H_{FC} = +10 kOe) from 375 K are represented in Figs. (a)-(c). The insets display the full-range hysteresis-loops within ±10 kOe. In Figure (d) the evolution of the exchange-bias field with respect to the temperature for as-quenched and annealed ribbons are plotted. Dashed lines are guides to the eyes.

To explore the low temperature magnetism of the $Ni_{50.0}Mn_{36.5}Sn_{13.5}$ for the three samples, we have performed FC hysteresis loops measurements at low temperatures. In the insets of the Figure 3 (a)-(c) are represented the *M(H)*hysteresis loops measured at 10 K from -10 kOe to +10 kOe after FC at +10 kOe from 375 K. The FC hysteresis loops, which are plotted in Figs. 3 (a)-(c) from -5 kOe to +5 kOe, shift to negative field values for the as-quenched and for the two annealed ribbons, which shows EB effect for the three samples. The EB field (H_E) and coercivity field (H_C) were evaluated

using $H_E = -(H_1 + H_2)/2$ and $H_C = |H_1 + H_2|/2$, where H_1 and H_2 are the left and right coercive fields at which the magnetization equals to zero, respectively. Fig.3 (d) shows the H_E dependence with respect to temperature. In fact, the H_E values decrease with increasing the temperature for the three ribbons, which, indeed, reveals a weakening of the FM-AFM coupling. At 10 K, in Fig. 3(a)-(c), H_E is around 170 Oe, 165 Oe and 182 Oe for the as-quenched, the Ann 923 K and the Ann 1073 K, respectively. These values are in good agreement with other Ni–Mn–Sn systems of similar composition [5, 13] and reveals that H_E remains unchanged by the annealing treatment. In addition, H_C diminishes for the annealed ribbons, as is clearly shown in the Figs. 3 (a)-(c). This behavior could be associated with the increasing of the grain size after annealing treatments, which, indeed, has been observed in the microstructure of the studied ribbons (this is not shown in this work).

Conclusion

The influence of high-temperature quenching treatments on both martensitic transformation and exchange-bias effect has been studied in the $Ni_{50.0}Mn_{36.5}Sn_{13.5}$ Heusler alloy ribbon. We show that the martensitic transformation shifts towards higher temperatures in consequence of the annealing treatment. Furthermore, from the *M(H)* hysteresis loops recorded at different temperatures, we observe an increase of H_E field with decreasing temperature for the three alloy ribbons, which is attributed to the coexistence of FM-AFM exchange interactions in Ni–Mn–Sn alloys ribbons. On the other hand, H_E is not affected by the annealing treatments performed in this work, whilst H_C decreases as a result of the key role played by AFM ordering in the martensitic phase in annealed samples.

Acknowledgements

Financial support under Spanish MINECO research Projects MAT2013-48054-C2-2-R and MAT2013-4731-C2-1-P, and under Russian Science Foundation, Grant No. 14-22-00279 is acknowledged. Scientific support from the University of Oviedo SCT's is also recognized. L. G.-L. thanks to MICINN for a FPI grant. Technical and human support provided by SGIker (UPV/EHU, MICINN, GV/EJ, ERDF and ESF) and University of Oviedo SCT's is gratefully acknowledged.

References

[1]: R. Kainuma, Y. Imano, W. Ito, Y. Sutou, H. Morito, S. Okamoto, O. Kitakami, K. Oikawa, A. Fujita. T. Kanomata, K. Ishida, *Nature* (London) **439** (2006), 957.
[2]: T. Krenke, E. Duman, M. Acet, E. F. Wassermann, X. Moya, L. Mañosa, A. Planes, *Nat. Mater.* **4** (2005) 450.
[3]: K. Koyama, H. Okada, K. Watanabe, T. Kanomata, R. Kainuma, W. Ito, K. Oikawa, K. Ishida, *Appl. Phys. Lett.* **89** (2006) 182510.
[4]: S. Singh, C. Biswas, *Appl. Phys. Lett.* **98** (2011), 212101.
[5]: M. Khan, I. Dubenko, S. Stadler, N. Ali, *J. Appl. Phys.* **102** (2007), 113914.
[6]: T. Krenke, M. Acet, E.F. Wassermann, X. Moya, Ll. Mañosa, A. Planes, *Phys. Rev. B* **72** (2005), 014412.
[7]: M. Acet, L. Mañosa, A. Planes, in: K.H.J. Buschow (Ed.), Handbook of Magnetic Materials, vol. 9, Elsevier, Amsterdam, 2011, p. 231.
[8]: J. Nogués, Ivan K. Schuller, *J. Magn. Magn. Mater*. **192** (1999) 203.
[9]: S Giri, M Patra, S Majumdar, *J. Phys.: Condens. Matter* **23** (2011) 073201.
[10]: V. D. Buchelnikov, P. Entel, S. V. Taskaev, V. V. Sokolovsky, A. Hucht, M. Ogura, H. Akai, M. E. Gruner, S. K. Nayak, *Phys. Rev. B* **78** (2008) 184427.
[11]: A.M. Aliev, A.B. Batdalov, I.K. Kamilov, V.V. Koledov, V.G. Shavrov, V.D. Buchelnikov, J. García, V.M. Prida, B. Hernando, *Appl. Phys. Lett.* **97** (2010), 212505.
[12]: S Esakki Muthu, N V Rama Rao, M Manivel Raja, D M Raj Kumar, D Mohan Radheep, S Arumugam, *J. Phys. D: Appl. Phys.* **43** (2010), 425002.
[13]: J. L. Sánchez Llamazares, H. Flores-Zúñiga, D. Ríos-Jara, C. F. Sánchez-Valdes, T. García-Fernández, C. A. Ross, C. García, *J. Appl. Phys.* **113** (2013), 17A948.